Eur Biophys J (1998) 27: 558–566

ARTICLE

A. Boccaccio · O. Moran · F. Conti

Calcium dependent shifts of Na^+ channel activation correlated with the state dependence of calcium-binding to the pore

Received: 1 December 1997 / Revised version: 25 March 1998 / Accepted: 27 March 1998

Abstract Calcium ions block the open configuration and antagonise the tonic binding of TTX to the closed state of sodium channels in very different ranges of extracellular concentration, $[Ca]_O$. We measured the open-state block in channels expressed in *Xenopus* oocytes by α-subunits from rat brain (rBIIa) or adult rat skeletal muscle (rSkM1). Recordings of instantaneous tail-currents from cell-attached macro patches show that the binding of Ca^{2+} to the blocking site has a dissociation constant of about 20 mM at 0 mV and senses about 30% of the membrane potential drop, whereas the concentration of half-inhibition of TTX-binding is less than 1 mM and voltage-insensitive. Assuming that both effects involve a single binding site, a simple model predicts that the state-dependency of the dissociation constant entails positive shifts of activation and faster kinetics of deactivation at increasing $[Ca]_O$. The shifts of activation measured for rBIIA and rSkM1 channels are comparable in size to those predicted by the model, which accounts also for the observed larger shifts of the rBIIA-mutant K226Q as a consequence of its reduced voltage-sensitivity. Shifts attributable to surface-charge screening effects seem smaller in the oocyte than in native cell-membranes. The experimental $[Ca]_O$-dependence of deactivation kinetics is also consistent with the model and with the idea that Ca^{2+}-binding changes to the same extent, but in opposite directions, the activation free-energies of both opening and closing transitions.

Key words Sodium-channel · Divalent cations · Ca^{2+}-dependent shifts · Ca^{2+}-block · Oocyte · Surface-charge

Introduction

Extracellular divalent cations modulate the properties of the sodium-channel by blocking the channel (Nilius 1988; Pusch 1990 a; Woodhull 1973) and by modifying its activation as if their binding stabilises its resting state (Frankenhaeuser and Hodgkin 1957; Hille 1992). The positive shift of the voltage dependence of activation at increasing extracellular Ca^{2+}-concentration, $[Ca]_O$, has been generally attributed exclusively to changes of the membrane surface potential due to the more efficient screening of fixed negative charges of the extracellular membrane face by the divalent cations (Frankenhaeuser and Hodgkin 1957; Hille 1968, 1975; Hille et al. 1975; McLaughlin et al. 1971). The surface charge theory can account for a whole variety of observed shifts, including those associated with pH changes or with changes in the concentrations of monovalent cations, by assuming several types of titratable groups and the additional neutralisation of pairs of adjacent acidic groups by complexation with divalent cations. However, there is no unique choice of the fitting parameters and no independent way of estimating them. By assuming one basic and two acidic surface groups with different densities and pK values and various dissociation constants for different divalent cations, Hille et al. (1975) found that a wide range of interdependent surface properties could yield a reasonable fit of the data.

Alternatively, Armstrong and Cota (1991) argued that the similarity between the increase of the activation-shifts with $[Ca]_O$ and the $[Ca]_O$-dependence of the activated sodium conductance suggests that calcium ions blocking the extracellular entrance of the sodium pore may also interfere directly with the gating mechanism of the channel. Calcium ions bind to the outer pore-vestibule of closed channels with high affinity, antagonising the binding of saxitoxin (STX) and tetrodotoxin (TTX) at submillimolar concentrations (Conti et al. 1996; Doyle et al. 1993), whereas the data reported here and in previous works on various preparations (Armstrong and Cota 1991; Pusch 1990 a; Woodhull 1973) show that the block of open channels occurs at much higher $[Ca]_O$ values, with dissociation constants of tens of mM at 0 mV. If the affinity for Ca^{2+} in the open state is lower, then the transition from the closed to the open conformation is less favoured when the channel is occupied by a calcium ion. So far there has been no

A. Boccaccio · O. Moran · F. Conti (✉)
Istituto di Cibernetica e Biofisica CNR, Via De Marini 6,
I-16149 Genova, Italy
e-mail: conti@barolo.icb.ge.cnr.it

theoretical evaluation of how this effect could influence the voltage-dependence of the activation of sodium currents. In this paper we develop a simple theory of the phenomenon and compare it with our measurements of Ca^{2+}-block and activation shifts of sodium channels expressed heterologously in *Xenopus* oocytes. We shall argue that most of the shifts observed in this preparation may result from the state-dependence of the interaction of Ca^{2+} with the channel protein.

Methods

Measurements were performed on α-subunits of sodium channels from rat brain (rBIIA; Noda et al. (1986)) or from adult rat skeletal muscle (rSkM1; Trimmer et al. (1989)) expressed by *Xenopus laevis* oocytes previously injected with the appropriate cRNA. In some experiments rSkM1-channels were co-expressed with the rat brain β1-subunit (Isom et al. 1992) in order to reduce the slowly inactivating mode of these channels (Patton et al. 1994). In general, the slow mode of both rBIIA and rSkM1 channels was suppressed using conditioning depolarisations (Moran et al. 1977). The cRNA's were transcribed *in vitro* from the recombinant plasmids using a commercial kit (mMessage mMachine, Ambion, USA). The oocytes were injected with 6 to 25 ng of cRNA and incubated for 2 to 8 days at 18 °C in Barth's solution. Sodium currents were measured from cell-attached membrane macro-patches using standard patch-clamp amplifiers (EPC-7, List Electronic, Germany; or Axopatch 200c, Axon Instruments, USA) (Stühmer 1992). The silicone-coated, fire-polished patch pipettes, from aluminium-silicate glass (Hilgemberg, Germany), were filled with extracellular solutions containing various fixed-osmolarity combinations of NaCl (117.5 to 102.5 mM) and $CaCl_2$ (0.2 to 10 mM) plus 2.5 mM-KCl and 10 mM-HEPES at pH = 7.4. The pipette resistance was between 0.6 and 1.2 MΩ. During the measurements the oocytes were maintained in a bathing solution with the following composition (in mM): KCl 120, TRIS-Cl 20, EGTA 5, pH 7.3. In this high-K^+ solution the cell potential was close to zero (±2 mV) and the membrane potential across the patch, V, was assumed to be just opposite to the pipette potential. The output of the patch clamp amplifier was filtered with a home-made low-pass four-pole Bessel filter, or with the built-in filter of the Axopatch amplifier, with a cut-off frequency of 20 or 50 kHz. Data were sampled at 100 or 200 kHz. Stimulation and acquisition protocols were controlled by the software package Pulse-PulseFit (Heka, Germany) running on a Macintosh microcomputer with a 16 bit AD/DA interface (ITC-16, Instrutech, USA). Linear current responses were measured from sub-threshold stimulations and digitally subtracted. All experiments were done at a controlled temperature of 15 ± 1 °C. For the off-line data analysis, including iterative model-fitting procedures, we used purpose-made programs written in the meta-language Igor (Wavemetrics, USA).

Results

Analysis of Ca-block of open channels

The voltage-dependence of the open-channel current can be evaluated from the instantaneous tail-currents measured from macroscopic current records. Patches yielding large currents (>400 pA of maximum peak current) are stimulated with a fixed pre-pulse to a potential V_{pp} that causes the opening of a large fraction of channels followed by steps to various tail potentials, V. The current, I, driven at V through the channels that are open at the end of the prepulse is estimated by extrapolation of the initial time course after the step. Sample records from two such experiments on rSkM1 at $[Ca]_O$ = 0.2 mM and $[Ca]_O$ = 20 mM are shown in Figs. 1A and 1B.

Each panel shows the pulse protocol (top), the current recordings on a full time scale (middle) and a time expansion of the same records near the onset of the tail voltage step (bottom). In both experiments the prepulse yielded about 90% activation of the peak sodium conductance, although V_{pp} was 30 mV more positive at $[Ca]_O$ = 10 mM owing to the calcium induced shift of activation discussed later (see Fig. 3). As shown in the bottom part of Figs. 1A and 1B, the kinetics of tail current relaxations for potentials less negative than 30 mV below V_{pp} are relatively slow. In these cases the initial tail current can be determined by linear extrapolation to the time, t_0, needed to reach about 90% of the current jump for steps to the reversal potential. For more negative potentials the tail currents were well fitted by single exponential relaxations at any time later than t_0 plus the reciprocal of the filter cut-off frequency and the initial current was determined by extrapolating these exponential fits to the time t_0. The most noticeable feature of the data of Fig. 1 is that, in contrast with its monotonic increase for more negative voltages in low $[Ca]_O$, the absolute value of the initial tail current in the high $[Ca]_O$ solution is smaller at –100 mV than at –60 mV. Another important observation is that the kinetics of tail deactivation at hyperpolarising potentials are much faster in the high $[Ca]_O$ solution.

Figure 2A shows tail I-V plots from the experiments of Figs. 1A and 1B, and from a similar measurement on another patch at $[Ca]_O$ = 1.8 mM. For comparison, since the amplitude of the tail currents depends on the number of channels in the patch and on the amount of activation at the end of the pre-pulse, the currents at $[Ca]_O$ = 0.2 mM and $[Ca]_O$ = 10 mM have been scaled to yield approximately the same slope conductance as those at $[Ca]_O$ = 1.8 mM near the reversal potential. It is seen that the I-V relation at negative potentials becomes progressively more strongly rectifying at increasing $[Ca]_O$. A rectification larger than expected from the difference in Na^+-concentration across the patch is also detectable at positive potentials owing to the voltage-dependent block by some uncontrolled level of intracellular Mg^{2+} (Lin et al. 1991; Pusch 1990b; Pusch et al. 1989). However, a much stronger rectification is seen for V < –30 mV at $[Ca]_O$ =

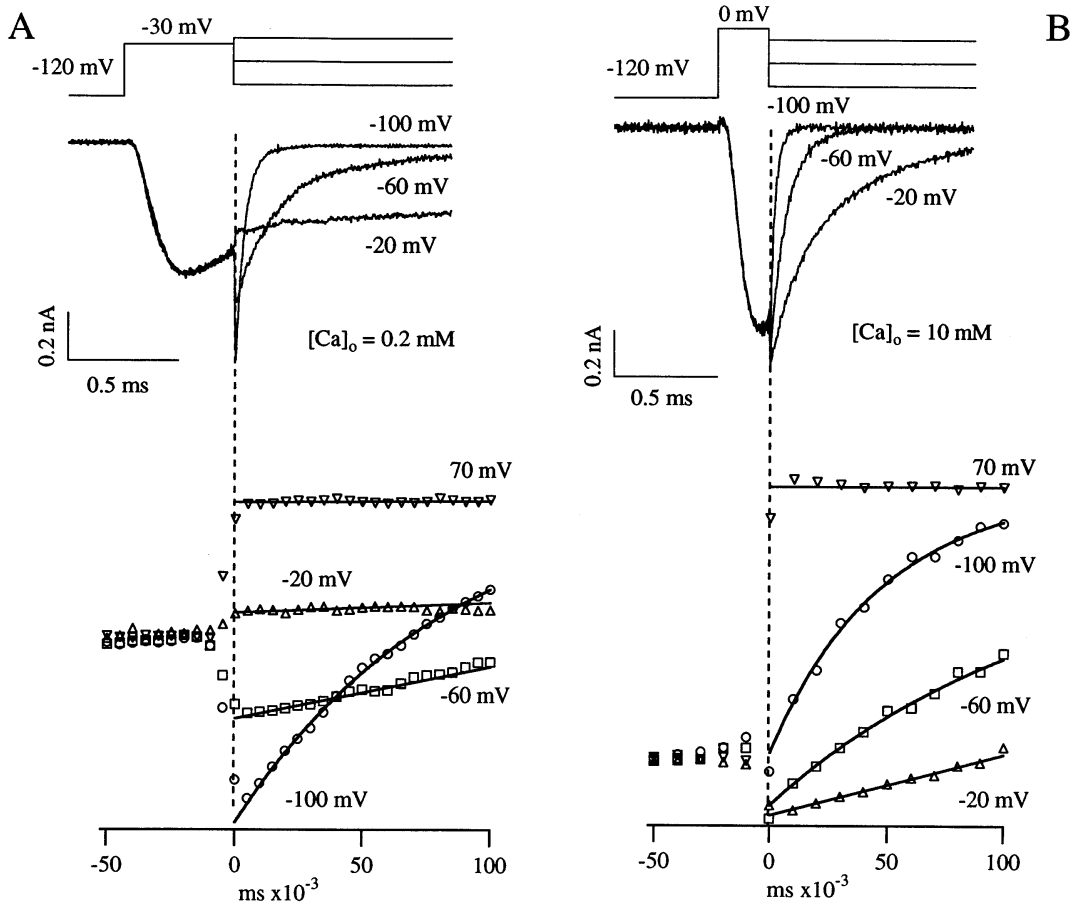

Fig. 1A, B The effect of extracellular Ca^{2+} on the tail current relaxations of rSkMμ1 channels. Representative records from similar experiments on two different cell-attached patches obtained with pipette-solutions containing $[Ca]_O$ = 0.2 mM (**A**) or with $[Ca]_O$ = 10 mM (**B**). Each panel shows the double-step protocol in the *upper part* and the current records on a full time scale in the *middle section*. The *bottom parts* show the same recordings near the onset of the tail voltage step on a very expanded time scale, to illustrate the method of measurement of deactivation kinetics and "instantaneous" tail currents. The vertical dashed lines show the effective time of tail onset, t_0, at which the tail current for steps to the reversal potential (~70 mV, in this case) is reduced to about 10% of its initial value. In these recordings, obtained with a bandwidth of 50 kHz, t_0 lagged the first visible tail change by 2 sampling intervals, i.e. 20 μs. Initial values of slowly relaxing tail currents were measured by linear extrapolation to t_0. For more negative potentials (e.g. at –100 mV in **A** and at –100 and –60 mV in **B**) the extrapolation of the tail currents to t_0 was obtained from single-exponential fits that also yielded the time constant of deactivation, τ_d

1.8 and 10 mM owing to the voltage-dependent block of the open channel by Ca^{2+}. In the case of $[Ca]_O$ = 10 mM the I-V relationship has a negative slope-conductance for V < –50 mV. In order to describe quantitatively the effect of calcium block we fitted tail I-V measurements according to the relation:

$$I(V) = \frac{I_0(V)}{1 + \frac{[Ca]}{K_O^{(0)}} \exp\left(-\frac{V}{v_b}\right)} \qquad (1)$$

where $K_O^{(0)}$ represents the dissociation constant of Ca^{2+} from the blocking site at V = 0, v_b is the e-fold voltage-sensitivity of Ca^{2+}-binding and $I_0(V)$ is the sodium current expected in the absence of calcium block. We assumed also the $I_0(V)$ is adequately described by the Goldman-Hodgkin-Katz equation (Hille 1992):

$$I_0 = \Gamma V \frac{\exp\left(-\frac{FV_{rev}}{RT}\right) - \exp\left(-\frac{FV}{RT}\right)}{1 - \exp\left(-\frac{FV}{RT}\right)} \qquad (2)$$

where V_{rev} is the reversal potential of the sodium currents and Γ is the asymptotic cord-conductance in the limit $V \to (-\infty)$. For each experiment in a given patch and $[Ca]_O$ conditions tail I-V plots were fitted by the combined Eqs. (1) and (2) to obtain estimates of the four parameters $K_O^{(0)}$, v_b, Γ and V_{rev}. The last two parameters varied widely from patch to patch, because Γ is a scaling factor mainly determined by the number of channels in the patch and by the amount of activation at the end of the pre-pulse, and because V_{rev} depends on the amount of sodium present in the oocyte cytoplasm. For convenience of presentation, the three experiments illustrated in Fig. 2 were chosen from patches that had approximately the same value of V_{rev} (~70 mV), and the currents at $[Ca]_O$ = 0.2 mM and $[Ca]_O$ = 10 mM were scaled to those at $[Ca]_O$ = 1.8 mM according to the estimates of Γ.

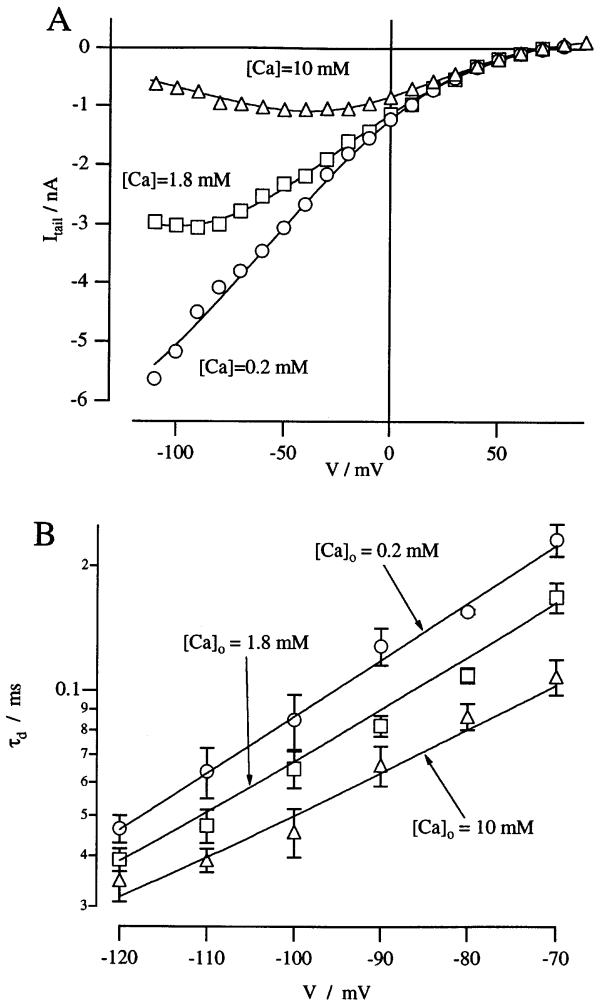

Fig. 2A Plots of the initial tail currents vs tail potential from the experiments of Fig. 1 and from a similar experiment with $[Ca]_O$ = 1.8 mM. The scale of the ordinates is for the 1.8 mM data. For the sake of comparison, the currents at $[Ca]_O$ = 0.2 mM and $[Ca]_O$ = 10 mM were scaled to yield approximately the same conductance near the reversal potential (~+70 mV) according to the different estimates of Γ from the fit of each experiment with Eqs. (1) and (2). The continuous lines through the data at $[Ca]_O$ = 1.8 mM and at $[Ca]_O$ = 10 mM show such least-squares fits, obtained, respectively, for $K_O^{(0)}$ = 19 mM, v_b = 48 mV and for $K_O^{(0)}$ = 20 mM, v_b = 38 mV. The line through the data at $[Ca]_O$ = 0.2 mM is the best fit for $K_O^{(0)}$ and v_b fixed to their mean estimates of 22 mM and 45 mV (Table 1). **B** $[Ca]_O$-dependence of the time constant, τ_d, of the exponential deactivation of rSkM1 channels for tail potentials between –120 and –70 mV. The plots show mean estimates (± s.d) from various experiments on different cell-attached patches with $[Ca]_O$ = 0.2 (n = 3), $[Ca]_O$ = 1.8 (n = 4) and $[Ca]_O$ = 10 mM (n = 3). The decrease of τ_d with $[Ca]_O$ is significantly more pronounced at less negative potentials and cannot be described by a simple positive shift of the voltage-dependence of deactivation kinetics. The *solid lines* through the data are best fits with Eqs. (9)–(11) according to the model described in Theory, obtained for $\beta_0(0) = 444\ s^{-1}$, z_d = 0.8, $\delta_i \approx \delta_e \approx 0.49$

The continuous lines through the inward-current data for $[Ca]_O$ = 1.8 mM and for $[Ca]_O$ = 10 mM are least-squares fits with Eqs. (1) and (2) obtained, respectively, for $K_O^{(+)}$ = 19 mM and v_b = 48 mV, and for $K_O^{(0)}$ = 20 mM and v_b = 38 mV. The data for $[Ca]_O$ = 0.2 mM could not be used to get independent estimates of $K_O^{(0)}$ and v_b, because at this low concentration the blocking effect of calcium ions is expected to exceed 20% only at voltages more negative than –110 mV. The line fitting these data in Fig. 2 was obtained by fixing $K_O^{(0)}$ and v_b to their mean estimated values ($K_O^{(0)}$ = 22 mM; v_b = 45 mV) from measurements at higher $[Ca]_O$ (Table 1). Since the correction introduced in this case by the blocking effect is very small, the goodness of the fit validates the use of Eq. (1) for the description of the currents through calcium-free channels.

Table 1 Parameters of the block by Ca^{2+} of open Na-channels

Phenotype	$K_O^{(0)}$/mM	v_b/mV	n
rBIIA	19 ± 7	40 ± 6	6
rSkM1	22 ± 7	45 ± 7	11
(*) rBIIA	14 ± 6	28 ± 7	
(*) rBIIA–K226Q	15 ± 4	34 ± 5	

* Estimates from the single-channel data of Pusch (1990a) at $[Ca]_O$ = 1.8 mM, using Eq. (1) for V = 0 and V = –50 mV

As in the examples of Fig. 2A, the estimates of $K_O^{(0)}$ and v_b obtained from experiments on rSkM1 channels at $[Ca]_O$ = 1.8 mM (n = 5), $[Ca]_O$ = 5 mM (n = 3), or $[Ca]_O$ = 10 mM (n = 3), did not show any systematic $[Ca]_O$-dependence, validating the analysis of the $[Ca]_O$-dependence of the block according to Eq. (1). Table 1 summarises our results for rSkM1 channels and for 6 experiments on rBIIA channels at $[Ca]_O$ = 1.8 mM. It is seen that the mean estimates of $K_O^{(0)}$ and v_b for the two isoforms are in very good agreement, as expected from the fact that both channels should have the same pore structure. There is also a fair agreement between our Ca^{2+}-block parameters and those estimated from single-channel recordings by Pusch (1990a) for rBIIA and for its point mutation K226Q. For later analysis we assumed that the binding of Ca^{2+} to the open pore of rSkM1, rBIIA, and K226Q is characterised by $K_O^{(0)}$ = 21 mM and v_b = 42 mV.

Figure 2B illustrates the other major effect of extracellular calcium on tail current relaxations. The figure shows plots of the mean estimates of the time constant of the exponential tail deactivation, τ_d, for tail potentials between –120 and –70 mV. The data are from experiments on rSkM1 channels at $[Ca]_O$ = 0.2, $[Ca]_O$ =1.8 and $[Ca]_O$ = 10 mM. The most obvious effect of increasing $[Ca]_O$ is a systematic decrease of τ_d that is progressively more pronounced at less negative potentials: e.g. the ratio between the values of τ_d at $[Ca]_O$ = 0.2 mM and $[Ca]_O$ = 10 mM increases monotonically from 1.4 at –120 mV to 2.2 at –70 mV. The last feature cannot be explained by a general positive shift of the effective voltage sensed by the gating structures of the channels, as expected by the mere screening or neutralisation of the membrane surface charge at increasing $[Ca]_O$. The solid lines through the data of Fig. 2B show the expectations of a model discussed later that assumes that the presence of a bound calcium ion interferes with gating.

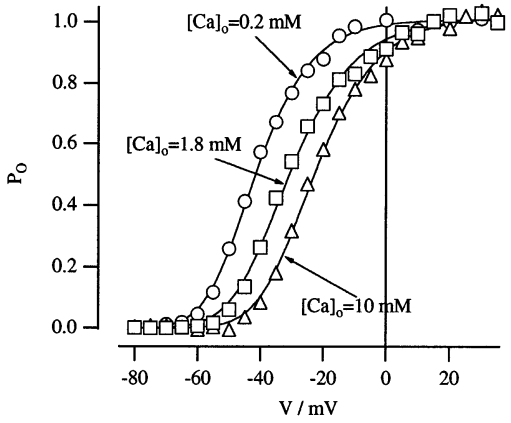

Fig. 3 Voltage-dependence of sodium-channel activation measured in the same experiments of Fig. 1. The *solid lines* are least-squares fits of the data according to Eq. (3) with: v_s = 8.5 mV, $V_{1/2}$ = –41.5 mV ($[Ca]_O$ = 0.2 mM); v_s = 9.9 mV, $V_{1/2}$ = –30.5 mV ($[Ca]_O$ = 1.8 mM); v_s = 9.6 mV, $V_{1/2}$ = –22.5 mV ($[Ca]_O$ = 10 mM)

Analysis of Ca-effects on activation

Following the classical analysis of Hodgkin and Huxley (1952) the voltage-dependence of the activation of sodium channels is described in terms of the ratio $I_{peak}/(V - V_{rev})$, where I_{peak} denotes the peak current in response to the voltage step to V. A better estimate of the activation probability, P_O, particularly at high $[Ca]_O$ values, should account for the non-linearity of the open-channel current by normalising I_{peak} to the measured instantaneous I-V relationships. Activation curves obtained in this way for the same experiments of Fig. 2 A are shown in Fig. 3. We found that other conceptual improvements of P_O estimates, e.g. replacing I_{peak} with the extrapolation of the inactivation decay, do not change significantly the two principal parameters of the activation curve, whose main characteristics are described by a simple Boltzmann relation:

$$P_O(V) = \frac{1}{1 + \exp\left(\frac{V_{1/2} - V}{v_s}\right)} \qquad (3)$$

where $V_{1/2}$ is the half-activation voltage and v_s is a slope factor characteristic the steepness of $P_O(V)$ at $V = V_{1/2}$. Least-squares fits of the data according to Eq. (3) are shown in Fig. 3 by solid lines. They were obtained for similar values of v_s (between 8.5 and 9.9 mV), with $V_{1/2}$ increasing with $[Ca]_O$ from –42 mV at $[Ca]_O$ = 0.2 mM to –23 mV at $[Ca]_O$ = 10 mM. The rigthward shift of sodium activation curves upon increasing $[Ca]_O$ is a well known effect (Frankenhaeuser and Hodgkin 1957; Hille 1968, 1975; Hille et al. 1975).

Equation (3) has a rigorous mechanistic interpretation only in the case of two-state channels, whereas it is well known that sodium channels have a multiplicity of closed states. However, although it would yield a better description of the foot of the activation curve, fitting the data according to the third power of the Hodgkin-Huxley (1952) activation parameter *m* would not change significantly the

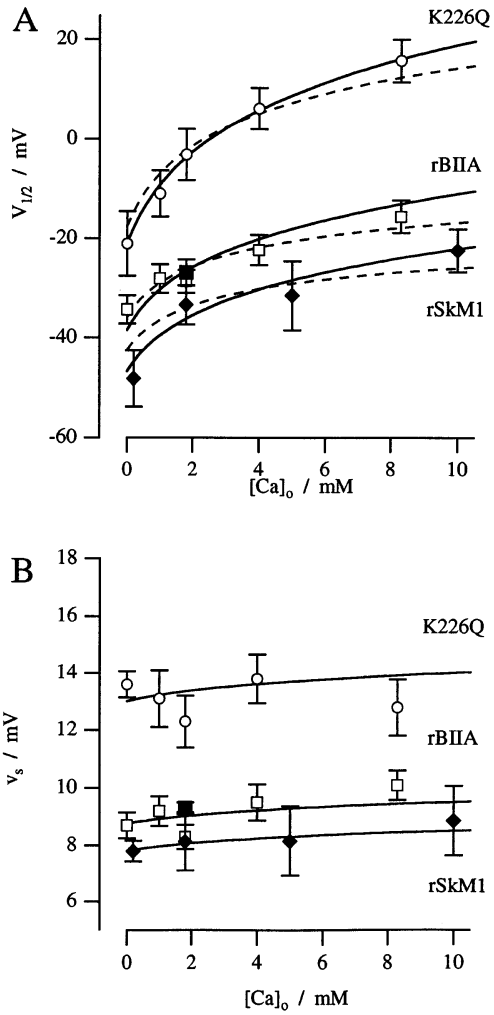

Fig. 4 Plots of the sodium-channel activation parameters $V_{1/2}$ (**A**) and v_s (**B**) as a function of $[Ca]_O$. Our present data for rSkMμ1 and rBIIA channels (*filled symbols*) are plotted together with data from Pusch (1990a) for rBIIA (*open squares*) and for its mutant K226Q (*open circles*). The dashed lines in **A** and the *solid lines* in **B** are least-squares fits according to the pure state-dependent model, Eqs. (7) and (8). The *solid lines* in **A** are better fits including shifts of the half-activation voltage due to the pure Ca^{2+}-screening (no binding) of charged groups on the outer membrane surface of the oocyte. The groups are of the same type but have only 40% of the surface density hypothesised by model II of Hille et al. (1975). In standard Ringer's solution the estimated free surface-charge and surface potential are –0.3 e/nm^2 and –47 mV

estimates of the mid-voltage and of the maximum slope. The data of Pusch (1990a) that we discuss later were given in terms of the fitted HH parameters V_m and z_m, characterising the equilibrium voltage and the valence of the *m* "gating particle". It is easily shown that these quantities can be converted to $V_{1/2}$ and v_s estimates through the relations (T=15 °C): $V_{1/2}/mV = V_m/mV + 33.4/z_m$; $v_s/mV = 20.1/z_m$.

Plots of our mean estimates of the activation parameters for rSkM1 as a function of $[Ca]_O$ are shown in Fig. 4, together with similar data from Pusch (1990a) for rBIIA and for its mutant K226Q (Stühmer et al. 1989). It is seen that rBIIA and rSkM1 have practically the same v_s, i.e. identical voltage-sensitivities. The half-activation voltage

of rSkM1 is about 8 mV more negative thant hat of rBIIA, but in both cases the increase with $[Ca]_O$ is about the same. Much greater differences characterise the K226Q mutation. As originally reported by Stühmer et al. (1989), this mutant has a marked positive shift of $V_{1/2}$ (by about 25 mV at $[Ca]_O$ = 1.8 mM) and a decreased voltage sensitivity, shown in Fig. 4B as a roughly 50% increase of v_s. A further peculiarity of K226Q, noticed by Pusch (1990a), is a marked increase of sensitivity to $[Ca]_O$ changes: changing $[Ca]_O$ from 0 to 8 mM shifts the mean $V_{1/2}$ of K226Q by about 35 mV, almost twice as much as in the wild type rBIIA (~19 mV) or in rSkMμ1 (~22 mV). The solid lines through the various sets of data in Fig. 4 were drawn according to the theory described below, which attributes a major portion of the $[Ca]_O$-dependent shifts to the state-dependency of calcium binding to the ion pore.

Theory

Disregarding inactivation and assuming a single open state (see e.g. Horn and Vandenberg 1994) the voltage dependence of the activation of sodium currents can be described by the scheme:

$$\{C\} \underset{\beta(V)}{\overset{\alpha(V)}{\rightleftharpoons}} O \qquad \text{Scheme [1]}$$

where O is the open state, {C} represents the set of possible closed states, $\alpha(V)$ and $\beta(V)$ are the equilibrium rates of opening and closing transitions, related to the open-state equilibrium probability, $P_O(V)$, by:

$$\frac{\alpha(V)}{\beta(V)} = \frac{P_O(V)}{P_{\{C\}}(V)} = \frac{P_O(V)}{1 - P_O(V)}.$$

It is easily verified that by approximating the voltage-dependence of $P_O(V)$ with Eq. (3) we imply that:

$$\frac{\alpha(V)}{\beta(V)} = \exp\left(\frac{V - V_{1/2}}{v_s}\right) \qquad (4)$$

Apart from effects of surface-charge screening that change the voltage drop experienced by the voltage-sensors of the channel, an additional dependence of $\alpha(V)$ and $\beta(V)$ on $[Ca]_O$ is expected *a priori* if the binding of Ca^{2+} interferes with transitions within {C} states or with {C} to O transitions. For simplicity, and in the absence of any experimental evidence that the calcium binding affinity of the closed channel is state dependent, we shall assume that only {C} to O transitions are affected by the presence of a bound calcium ion. We can then expand scheme [1] as:

$$\begin{array}{ccccc} & \{C_0\} & \underset{\beta_0(V)}{\overset{\alpha_0(V)}{\rightleftharpoons}} & O_0 & \\ \dfrac{[Ca]_O}{K_C} & \downarrow & & \downarrow & \dfrac{[Ca]_O}{K_O} \\ & \{C_1\} & \underset{\beta_1(V)}{\overset{\alpha_1(V)}{\rightleftharpoons}} & O_1 & \end{array} \qquad \text{Scheme [2]}$$

where the subscripts 1 and 0 indicate binding or not of a calcium ion, with dissociation constant K_C for all closed states and K_O for the open state. Disregarding Ca^{2+}-permeation and the probability of cyclic reactions driven by the Ca^{2+} free-energy gradient, the microscopic reversibility of scheme [2] requires that:

$$\frac{\beta_1(V)}{\alpha_1(V)} = \frac{K_O^{(0)}}{K_C} \exp\left(\frac{V}{v_b}\right) \frac{\beta_0(V)}{\alpha_0(V)} \qquad (5)$$

where the voltage dependence of K_O revealed by the open-channel block is introduced explicitly, whereas K_C is assumed to be voltage-independent on the basis of the analysis of TTX-Ca^{2+} interactions in the closed channel (Conti et al. 1996). Equation (5) implies that the free-energy difference between the open and closed states, $\Delta G = G_O - G_C = kT \times \ln(\beta/\alpha)$, is changed by the presence of a bound Ca^{2+} because of two effects: 1) the different interaction of the ion with the two conformations of the channel protein changes ΔG by $kT \times \ln(K_O^{(0)}/K_C)$; 2) the opening of the channel exposes the ion to a fraction $RT/(2Fv_b)$ of the membrane voltage drop and involves, therefore, an additional ΔG of $kT \times (V/v_s)$. Using Eq. (5) it is easily shown that scheme [2] reduces to scheme [1] if:

$$\frac{\alpha(V)}{\beta(V)} = \frac{\alpha_0(V)}{\beta_0(V)} \frac{1 + \dfrac{[Ca]_O}{K_O^{(0)}} \exp\left(-\dfrac{V}{v_b}\right)}{1 + \dfrac{[Ca]_O}{K_C}}$$

Expressing $\alpha(V)/\beta(V)$ and $\alpha_0(V)/\beta_0(V)$ according to Eq. (4) this relation becomes:

$$\exp\left(\frac{V - V_{1/2}}{v_s}\right) = \frac{1 + \dfrac{[Ca]_O}{K_O^{(0)}} \exp\left(-\dfrac{V}{v_b}\right)}{1 + \dfrac{[Ca]_O}{K_C}} \exp\left(\frac{V - V_{1/2}^*}{v_s^*}\right) \qquad (6)$$

where $V_{1/2}^*$ and v_s^* are the parameters that characterise the gating properties at $[Ca]_O$ = 0. Equation 6 cannot be identically verified at all voltages V, but this is not a major obstacle for our present analysis, which is only concerned with estimating $V_{1/2}$ and the slope parameter v_s. For that purpose we just need to impose in Eq. (6) the identity of the two members and of their derivatives at $V = V_{1/2}$. The first condition yields:

$$V_{1/2} = V_{1/2}^* + v_s^* \ln\left(\frac{1 + \dfrac{[Ca]_O}{K_C}}{1 + \dfrac{[Ca]_O}{K_O^{(0)}} \exp\left(-\dfrac{V_{1/2}}{v_b}\right)}\right). \qquad (7)$$

The second condition yields:

$$\frac{1}{v_s} = \frac{1}{v_s^*} - \frac{1}{v_b} \frac{1}{1 + \dfrac{K_O^{(0)}}{[Ca]_O} \exp\left(\dfrac{V_{1/2}}{v_b}\right)}. \qquad (8)$$

For given values of $K_O^{(0)}$, v_b and K_C, Eqs. (7) and (8) define implicitly $V_{1/2}$ and v_s as functions of $[Ca]_O$. In particular, Eq. (8) predicts a small monotonic increase of v_s with $[Ca]_O$ towards the asymptotic value:

$$v_s^{max} = \frac{v_b}{v_b - v_s^*} v_s^*$$

Likewise, Eq. (7) predicts a monotonic increase of $V_{1/2}$ with $[Ca]_O$ towards the asymptotic value:

$$V_{1/2}^{max} = V_{1/2}^* + v_2^{max}\left(\frac{V_{1/2}^*}{v_b} + \ln\frac{K_O^{(0)}}{K_C}\right)$$

Scheme [2] also predicts a simple $[Ca]_O$-dependence of the tail current kinetics at deactivating potentials, such that α_0 and α_1 are negligible with respect to β_0 and β_1. At these voltages the open channel probability as expected to decay exponentially with a time constant, τ_d, given by the relation:

$$\frac{1}{\tau_d(V)} = \beta_0(V)\frac{K_O(V) + [Ca]_O\frac{\beta_1(V)}{\beta_0(V)}}{K_O(V) + [Ca]_O} \qquad (9)$$

where $\beta_0(V)$ is the decay rate of the tail currents in zero calcium and where $\beta_1(V)/\beta_0(V)$ is the factor by which the rate constant of the closing transition is increased in the presence of a bound calcium ion. This factor is determined by the calcium-induced decrease in the free energy of activation of the closing transition which should be a fraction of the increase in ΔG of the $\{C\} \rightarrow O$ reaction. Therefore, according to Eq. (5), we expect for $\beta_1(V)/\beta_0(V)$ the following expression:

$$\frac{\beta_1(V)}{\beta_0(V)} = \exp\left(\delta_i \ln\frac{K_O^{(0)}}{K_C} + \delta_e\frac{V}{v_b}\right) \qquad (10)$$

where δ_i and δ_e represent the fraction of the two contributions to the change in ΔG, discussed in connection with Eq. (5), afforded by the closing transition. If a bound calcium ion has equal and opposite effects on the activation barriers for the opening and closing transitions, we expect $\delta_i = \delta_e = 0.5$. Notice that Eq. (9) predicts that if β_1/β_0 is voltage independent ($\delta_e = 0$) the exponential dependence of K_O on V would make the ratio of the low- to high-$[Ca]_O$ values of τ_d decrease with V, whereas this tendency is counteracted for $\delta_e > 0$ by the exponential increase of β_1/β_0 so that the overall effect on τ_d ratios may be just opposite.

In order to evaluate the predictions of the above simple model, we must use some reasonable value of K_C. The only experimental data providing estimates for this parameter are obtained from studies of the antagonistic action of Ca^{2+} on the binding of TTX and STX, whose receptor pocket likely includes the Ca^{2+}-binding site. In the sodium channels of reconstituted vesicles from native cardiac and brain tissue the binding of radioactive labelled STX is antagonised at increasing extracellular Ca^{2+}-concentrations (Doyle et al. 1993). Although the membrane potential of these preparations is undefined, it is fair to assume that the data relate to closed configurations because the steady-state open probability of native sodium channels is very low at any voltage. At the site of competition, Doyle et al. (1993) measured a dissociation constant for Ca^{2+}-binding, $K_{Ca} \sim 0.34$ mM, whereas for Na^+-binding the estimate is $K_{Na} \sim 34$ mM (Doyle et al. 1993; Weigele and Barchi 1978). A comparable value, $K_{Ca} \sim 0.16$ mM, was estimated for the binding of Ca^{2+} to resting rBIIA channels from measurements of the use-dependence of TTX-block by attributing the effect to the removal of the inhibition by Ca^{2+} (Conti et al. 1996). The latter analysis also indicated that K_{Ca} is fairly independent of voltage, as also suggested by the close agreement between the estimate of Conti et al. (1996) for $V < -100$ mV and that of Doyle et al. (1993) for depolarised conditions.

A number of other observations give circumstantial support to the idea of a high affinity binding of Ca^{2+} to closed channels. The antagonism between Ca^{2+} and cations occupying the cytoplasmic side of the sodium pore may explain the apparent interaction of TTX with local anaesthetics (Cahalan and Almers 1979) or with thiazin dyes (Armstrong and Croop 1982) if one assumes that TTX reduces a normally high probability of calcium binding, thereby relieving the repulsion of the drugs. Also the modification of gating currents by STX or TTX (Heggeness and Starkus 1986; Keynes et al. 1991) might arise indirectly from the displacement of Ca^{2+} by the toxins if the binding of Ca^{2+} interferes with gating, as proposed by Armstrong and Cota (1991) and supported by the present work. The above quoted effects are quite substantial in normal conditions. Therefore, if they are attributed to unbinding of Ca^{2+}, they are consistent with K_{Ca} values lower than the physiological $[Ca]_O$.

To compare the predictions of Eqs. (7) and (8) with our data we assumed $K_C = 0.72$ mM, a value derived using the estimate $K_{Ca} = 0.16$ mM obtained by Conti et al. (1996) for the oocyte preparation and taking into account that the effective dissociation constant is increased by the factor $(1 + [Na]/K_{Na})$ due to competition with Na^+. For the open channel parameters we assumed the mean estimates $K_O^{(0)} = 21$ mM and $v_b = 42$ mV as invariant characteristics of the three phenotypes of Fig. 4. We solved numerically Eqs. (7) and (8) searching for each set of data for one phenotype the values of $V_{1/2}^*$ and v_s^* yielding the minimum χ^2. The best fits obtained in this way are shown by dashed lines in Fig. 4A and by the continuous lines of Fig. 4B. It is clear that the mere inclusion of the state-dependent binding can account for most of the observed $[Ca]_O$-dependence of $V_{1/2}$. Also the tendency of the v_s measurements to increase with $[Ca]_O$ is consistent with the model, although this feature cannot be used in support of the model, owing to the large scatter of the data.

Our model does not exclude the possibility that a significant contribution to the shifts of $V_{1/2}$ may also arise from the decrease with $[Ca]_O$ of the negative surface potential at the outer surface of the oocyte membrane. Such contribution, supposedly identical for the three phenotypes of Fig. 3, was included by allowing $V_{1/2}$ to change with $[Ca]_0$ as expected from the screening of titratable surface

groups of the type postulated by Hille et al. (1975) for the frog node membrane. We did not assume, however, any specific binding of Ca^{2+} to the negative groups and we looked for best fits of the data of Fig. 4A by allowing the densities of the surface groups to be scaled by a common factor. As expected, adding the surface-charge correction significantly improved the fit of the data, as shown by the continuous lines of Fig. 4A. The improvement was insensitive to the type of surface-charge model used: the best scaling factor was 0.22 for the high-density model I of Hille et al. (1975), and was 0.4 for the lower density model II. At $[Ca]_O$ = 1.8 mM both models yield –0.3 *e*/nm^2 as the best estimate of the free surface-charge density and a surface potential of about –47 mV. After including the effect of surface-charge screening we estimate that the contribution of state-dependence effects to the total shift observed upon raising $[Ca]_O$ from 0.2 to 10 mM is 66% for rSkM1, 69% for rBIIA and 79% for the mutant K226Q.

The model discussed above also provides a good description of the $[Ca]_O$-dependence of deactivation kinetics. The solid lines through the data of Fig. 2B were obtained from the least-squares fit to Eqs. (9) and (10) assuming a small $[Ca]_O$-dependent shift of both $\beta_0(V)$ and $\beta_1(V)$ due to the above estimated surface charge screening (from 0.3 mV at $[Ca]_O$ = 0.2 to 8.0 mV at $[Ca]_O$ = 10 mM), and a voltage dependence of $\beta_0(V)$ of the type:

$$\beta_0(V) = \beta_0(0)\exp\left(-z_d \frac{FV}{RT}\right) \qquad (11)$$

where z_d is the gating charge of the closing transition. The best overall fit of the data of Fig. 2B and of similar data at $[Ca]_O$ = 5 mM (not shown) was obtained for $\beta_0(0)$ = 444 s^{-1}, z_d = 0.8, and $\delta_i \approx \delta_e \approx 0.49$. Thus, the effect of extracellular calcium on deactivation kinetics is consistent with Ca^{2+} changing by about the same extent (but in opposite directions) the free energy of activation of both the opening and the closing transition.

Discussion

We asked in this paper to what extent the different calcium-binding affinity of the sodium-channel in the open and closed states may account for the shifts of the sodium activation curve, that would be thus related to a direct influence of calcium on gating as proposed by Armstrong and Cota (1991). The model that we have used to estimate this effect assumes that the presence of a bound calcium ion in the outer vestibule or at the selectitivity filter of the channel modifies only the open-close transitions. Despite its oversimplification this model does show that a major portion of the $[Ca]_O$-dependent shifts observed for sodium channels expressed in oocytes is indeed consistent with the state-dependence of calcium binding estimated for the same preparation.

Although adding to the state-dependent model the shifts due to the screening of negative surface charges improves the fit of our data, this contribution seems rather low in comparison to other membrane preparations. In their study of the pituitary cell line GH3 Armstrong and Cota (1991) report shifts of $V_{1/2}$ by +27 mV and by +47 mV upon raising $[Ca]_O$ from 0.2 to 10 mM and 50 mM. From their activation curves and calcium-block data we roughly estimate for preparation their $V^*_{1/2} \sim -55$ mV, $v^*_s \sim 7$ mV, $K^{(0)}_O \sim 70$ mM and $v_b \sim 30$ mV. Assuming K_C = 0.55 at their sodium concentration of 80 mM, the shifts attributed by our model to the state-dependence of calcium binding are +16 mV and +22 mV, i.e. only 59% and 39% of those observed. We suppose that the density of surface charges in this preparation is higher and that the shifts due to their screening by Ca^{2+} are consequently larger and have a relative weight that increases consistently with $[Ca]_O$. A similar conclusion can be drawn for the frog node preparation, where changing $[Ca]_O$ from 0 to 20 mM at constant $[Na]_O$ = 140 mM shifts sodium activation by about +40 mV (Hille et al. 1975). For that system $V_{1/2} \sim 50$ mV, $v^*_s \sim 7$ mV, the block parameters are $K^{(0)}_O$ = 53 mM and $v_b \sim 48$ mV (Woodhull, 1973), and the corresponding shift predicted by our model with K_C = 0.64 mM is 20.5 mV, i.e. only 51% of that observed. The idea that the oocyte membrane has a lower density of negative surface charges is also supported qualitatively by the observation that the sodium channels expressed in this model membrane have a substantially less negative $V_{1/2}$ than in the native environment. At $[Ca]_O$ = 1.8 mM the $V_{1/2}$ of our rBIIA channels is about –30 mV as compared to values in the range –50 to –55 mV measured in the frog node or in GH3 cells. The larger depolarisation needed to activate the channels in the oocyte might just compensate a less negative surface potential on the outer membrane face.

A remarkable success of our model is the fair description of the substantially different shifts of K226Q and wild-type channels using a fixed set of parameters for the interaction of Ca^{2+} with the sodium pore. The invariance of the interaction with the open pore is directly supported by our measurements on rSkMμ1 and rBIIA which agree well with the Ca^{2+}-block properties of rBIIA and of mutant K226Q reported by Pusch (1990a). That rSkMμ1 and rBIIA have the same Ca^{2+}-binding properties in the closed state is supported by the fact that they show the same $[Ca]_O$-dependence of the use-dependent block by TTX (unpublished results). As for K226Q, it is unlikely that a point mutation at the cytoplasmic end of segment S4-I affects the binding properties of the extracellular pore domain. Our model explains the much larger shifts of mutant K226Q as a mere consequence of the lower voltage sensitivity and intrinsic shift of the activation curve. Ignoring state-dependent effects, the surface-charge theory could explain the phenotypic variation of the calcium shifts only by assuming a change of the extracellularly exposed charge near the voltage-sensing structures of the channel. Indeed, several charge mutations in the segments S4-I and S4-II show intrinsic shifts of activation that may be associated with a local change of the exposed charges on either side of the channel (Stühmer et al. 1989). In particular, the positive shift of mutant K226Q may result from the neutralisation of a pos-

itive charge normally exposed to the cytoplasmic side. However, such a change would not affect the charges on the extracellular face of the membrane and there is, therefore, no plausible explanation of the increased $[Ca]_O$-sensitivity of K226Q in terms of surface-charge effects.

The only essential assumption that we have used for modelling $[Ca]_O$ effects is that the binding of calcium ions to the outer pore of sodium channels is state dependent, quite regardless of the precise mechanism that causes such dependence. We have shown on purpose that even for the most simple case in which a bound calcium ion modifies only the open-close transitions we expect $[Ca]_O$ effects of a size comparable to those observed, but we cannot exclude the possibility that direct interactions of Ca^{2+} with the charged groups that are responsible for the voltage dependence of activation (voltage sensors) contribute to the state dependence of Ca^{2+}-binding. Likewise, speaking of a single Ca^{2+}-binding site might be inappropriate if the activation of a channel and/or the opening of its permeation pathway involve structural changes of the outer pore-mouth that effectively change the molecular configuration of the Ca^{2+}-binding pocket. Nevertheless, it is important to stress that our model is also consistent with the view that the voltage sensors of the sodium channel do not interfere with its outer-pore structure and that the opening does not modify the short-range Ca^{2+} binding interactions, because changes of the binding-energy of the order of those observed ($kT \ln(K_O^{(0)}/K_C) \approx 3.4\ kT$) may easily result from changes in long-range electrostatic interactions with other groups or regions of the channel protein that do not shape the binding pocket. Indeed, it is plausible that Ca^{2+} blocks the open pore at a site located just before the barrier of the pore selectivity filter and interacts from there with charged or polar structures that gate the cytoplasmic pore entrance and are likely distinct from the voltage-sensing structures that enable or disable their operation.

Acknowledgements We thank K. Imoto for providing rBIIA and rat brain β1 cDNA's, W. Agnew for providing the rSkM1 cDNA, M. Nizzari for helping us with the cRNA preparation, and E. Gaggero for technical assistance and the making of the Bessel filter. This work was supported by Telethon Grant 926.

References

Armstrong CM, Cota G (1991) Calcium ion as a cofactor in Na channel gating. Proc Natl Acad USA 88:6528–6531

Armstrong CM, Croop RS (1982) Simulation of Na channel inactivation by thiazin dyes. J Gen Physiol 641–662

Cahalan MD, Almers W (1979) Interactions between quaternary lidocaine, the sodium channel gates, and tetrodotoxin. Biophys J 27:39–56

Conti F, Gheri A, Pusch M, Moran O (1996) Use dependence of tetrodotoxin block of sodium channels: A revival of the trapped-ion mechanism. Biophys J 71:1295–1312

Doyle DD, Guo Y, Lusting SL, Satin J, Rogard RB, Fozzard HA (1993) Divalent cation competition with [^{3}H]saxitoxin binding to tetrodotoxin-resistant and -sensitive sodium channel: a two-site structural model of ion/toxin interaction. J Gen Physiol 101:153–182

Frankenhaeuser B, Hodgkin AL (1957) The action of calcium on the electrical properties of squid axons. J Physiol 137:218–244

Heggeness ST, Starkus JG (1986) Saxitoxin and tetrodotoxin. Electrostatic effects on sodium channel gating current in crayfish axons. Biophys J 49:629–643

Hille B (1968) Charges and potentials at the nerve surface: divalent ions and pH. J Gen Physiol 51:221–236

Hille B (1975) The receptor for tetrodotoxin and saxitoxin. Biophys J 15:615–619

Hille B (1992) Ionic channels of excitable membranes. Sinauer, Sunderland, Mass

Hille B, Woodhull AM, Shapiro BI (1975) Negative surface charge near sodium channels of nerve: divalent ions, monovalent ions, and pH. Phil Trans R Soc (Lon B) 270:301–318

Horn R, Vandenberg CA (1994) Statistical properties of single sodium channels. J Gen Physiol 84:505–534

Isom LL, De Jongh KS, Patton DE, Reber BFX, Offord J, Chaboneau H, Walsh K, Goldin AL, Catterall WA (1992) Primary structure and functional expression of the β_1 subunit of the rat brain sodium channel. Science 256:839–842

Keynes RD, Greeff NG, Forster IC, Bekkers JM (1991) The effect of tetrodotoxin on the sodium gating current in the squid giant axon. Proc R Soc (Lond B) 246:135–140

Lin F, Conti F, Moran O (1991) Competitive blockage of the sodium channel by intracellular magnesium ions in central mammalian neurones. Eur Biophys J 19:109–118

McLaughlin SGA, Szabo G, Eisenman G (1971) Divalent ions and the surface potential of charged phospholipid membranes. J Gen Physiol 58:667–687

Moran O, Nizzari M, Conti F (1997) Modal gating of sodium channels and possible physiological implications on hereditary myopathies. In: Torre V, Nicolls J (eds) Neuronal circuits and networks. Plenum Press, New York (in press)

Nilius B (1988) Calcium block of guinea-pig heart sodium channels with and without modification by peperazinnylidole DPI 201-106. J Physiol 399:537–558

Noda M, Ikeda T, Kayano T, Suzuki H, Takeshima H, Kurasaki M, Takahashi H, Numa S (1986) Existence of distinct sodium channel messenger RNAs in rat brain. Nature 320:118–192

Patton DE, Isom LL, Catterall WA, Goldin AL (1994) The adult rat brain β_1 subunit modifies activation and inactivation gating of multiple sodium channel α subunits. J Biol Chem 269:17640–17655

Pusch M (1990a) Divalent cations as probes for structure-function relationships of cloned voltage-dependent sodium channels. Eur Biophys J 18:327–333

Pusch M (1990b) Open-Channel block of Na^+ channels by intracellular Mg^{2+}. Eur Biophys J 18:317–326

Pusch M, Conti F, Stühmer Q (1989) Intracellular magnesium blocks sodium outward currents in a voltage- and dose-dependent manner. Biophys J 55:1267–1271

Stühmer W (1992) Electrophysiological recording of *Xenopus* oocytes. In: Rudy B, Iverson LE (eds) Method in enzymology: ion channels. Academic Press, London, pp 319–339

Stühmer W, Conti F, Suzuki H, Wang X, Noda M, Yagahi N, Kubo H, Numa S (1989) Structural parts involved in activation and inactivation of the sodium channel. Nature 339:597–603

Trimmer JS, Cooperman SS, Tomiko SA, Zhou J, Crean SM, Boyle MB, Kallen RG, Sheng Z, Barchi RL, Sigworth FJ, Goodman RH, Agnew WS, Mandel G (1989) Primary structure and functional expression of a mammalian skeletal muscle sodium channel. Neuron 3:33–49

Weigele JB, Barchi RL (1978) Saxitoxin binding to the mammalian sodium channel. Competition by monovalent and divalent cations. FEBS Lett 95:49–53

Woodhull AM (1973) Ionic blockage of sodium channels in nerve. J Gen Physiol 61:687–708